Dynamic and Reversible Decoration of DNA-Based Scaffolds

Nada Farag, Milan Đorđević, Erica Del Grosso, and Francesco Ricci**

Department of Chemistry, University of Rome Tor Vergata, Via della Ricerca Scientifica, 00133, Italy

E-mail: francesco.ricci@uniroma2.it

Abstract:

We demonstrate here an approach to achieve dynamic and reversible decoration of DNA-based scaffolds. To do this, we employ rationally engineered DNA tiles containing enzyme-responsive strands covalently conjugated to different molecular labels. These strands are designed to be recognized and degraded by specific enzymes (i.e., Ribonuclease H, RNase H or Uracil DNA Glycosylase, UDG) inducing their spontaneous de-hybridization from the assembled tile and replacement by a new strand conjugated to a different label. Multiple enzyme-responsive strands that specifically respond to different enzymes allow for dynamic, orthogonal, and reversible decoration of the DNA structures. As a proof-of-principle of our strategy, we demonstrate the possibility to orthogonally control the distribution of different labels (i.e., fluorophores and small molecules) on the same scaffold without crosstalk. By doing so we obtain DNA scaffolds that display different antibodies recognition patterns. Our approach offers the possibility to control the decoration of higher-order supramolecular assemblies (including origami) with several functional moieties to achieve functional biomaterials with improved adaptability, precision, and sensing capabilities.

Keywords: DNA nanotechnology, DNA repair enzyme, endoribonuclease enzymes, DNA tiles, self-assembly, functionalization, decoration

1. Introduction

Over the past three decades, many efforts have been dedicated to the use of biomolecules such as polysaccharides,[1,2] lipids,[3,4] and peptides[5,6] as building blocks for the fabrication of molecular polymers and nano or micron-scale structures.[7] A positive feature of these materials is that they can act as versatile molecular bio-scaffolds and be decorated with different ligands, recognition elements, and molecular labels to provide a variety of functionalities that can find applications in sensing,[8,9] bioimaging,[10] drug delivery,[11] and tissue engineering.[12] In this context, supramolecular amphiphilic peptide nanofibers have been, for example, employed as promising materials in the field of regenerative medicine.[13] Similarly, lipid-based scaffolds have been decorated with adhesion molecules or receptor-mediated recognition ligands to create materials that may be useful as drug carrier systems.[3,14] As the assembly of these structures usually proceeds through the formation of non-covalent reversible interactions, they can also be designed to undergo a change in their structural configuration or functionality in response to multiple chemical and environmental stimuli.[15,16] Rational and programmable control of these supramolecular functional bio-scaffolds remains, however, challenging, and it is often difficult to achieve higher-order organization of multiple labeling groups in a versatile and dynamic way.

Compared to other biomolecules employed for the self-assembly of structures and scaffolds, the use of synthetic DNA as a building block presents several advantages. First, the predictable and programmable nature of DNA-DNA base pairing allows the rational design of DNA-based structures with well-defined 2D and 3D geometry.[17,18] Second, the sequence-specific addressability of DNA strands together with the possibility to covalently attach different functional moieties on the backbone of a DNA oligonucleotide permit the controlled nanoscale decoration at specific locations on the DNA structure with several molecular labels. The above features have been successfully exploited in the last years to make DNA-based scaffolds decorated with a variety of different chemical and biological species such as antibodies,[19,20] signaling moieties,[21,22] aptamers,[23,24] virus capsids,[25,26] and proteins[27,28] that have found applications in bioimaging, drug delivery, and cancer therapeutics.[21,29,30] Despite the above examples clearly illustrate the versatility of synthetic DNA as building blocks to create molecular bio-scaffolds, the methods employed so far for the decoration of DNA-based assemblies often lack versatility and programmability, they are “static” and do not allow the replacement of the labels “on the fly” without prior structure disassembly. Developing novel approaches to control the decoration and labelling of DNA scaffolds with

multiple functional moieties in a dynamic way will allow for achieving functional biomaterials with improved adaptability, precision, and sensing capabilities.

Motivated by the above arguments, we demonstrate here a strategy to achieve dynamic and site-specific decoration of DNA-based scaffolds. To do so, we employed a model scaffold system DNA structure formed through the self-assembly of DNA tiles. More specifically, we have employed double-cross-over DNA tiles (DAE-E) formed through the hybridization of five different DNA strands.[31–33] These tiles display 4 single-stranded sticky ends (each of 5 nucleotides) that induce their spontaneous self-assembly into micron-scale hollow tubular structures (**Figure 1a**-b). It is possible to covalently conjugate to one of the tile-forming strands a molecular label (i.e., fluorophore, antigen, recognition element, etc.) (red circle) that will be thus homogenously distributed along the DNA-based structure. To achieve dynamic control of the decoration of such molecular scaffolds, we have rationally re-engineered the label-conjugated strand so that it can be enzymatically degraded by a specific enzyme. Upon enzymatic degradation, the strand spontaneously de-hybridizes from the assembled tile and can be replaced by a new strand conjugated to a different label (Figure 1c). Multiple enzyme-responsive strands that specifically respond to different enzymes can be designed to allow dynamic, orthogonal, and reversible decoration of the DNA scaffolds using multiple labels.

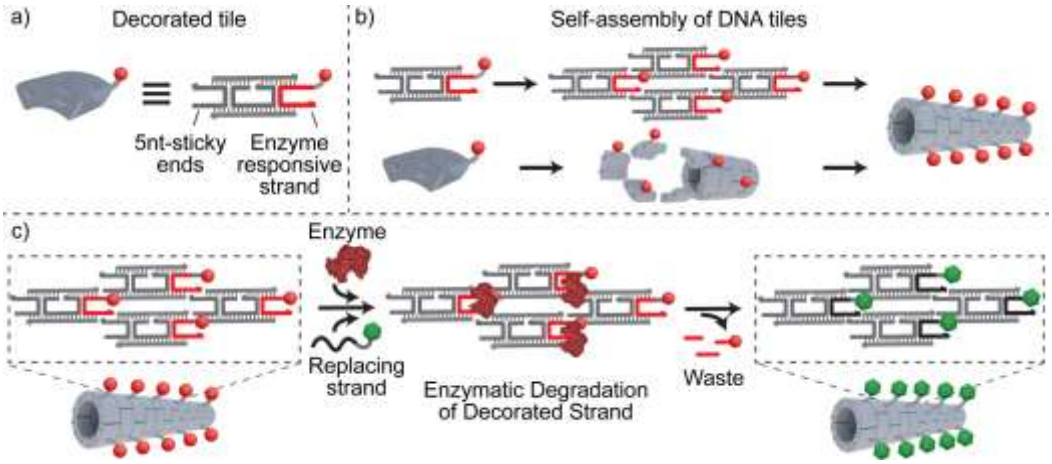

Figure 1. Dynamic decoration of DNA-based scaffolds. *a) Cartoon of the double-cross-over DNA tile (DAE-E) displaying the 4 sticky ends. The 5' end of one of the tile-forming strands (red) is covalently conjugated to a molecular label (i.e., fluorophore, antigen, recognition element, etc.) (red circle). DNA tiles are depicted here as LEGO®-like brick models where knobs and holes represent the four sticky ends. b) Self-assembly process of the DNA-based structure. c) In the presence of a specific enzyme, the red strand can be degraded and replaced by a new strand conjugated to a different label (green).*

2. Results and Discussion

2.1. RNase H-Driven Decoration Replacement in DNA-Based Scaffolds

As a first proof-of-principle of our strategy, we employed a label-conjugated RNA strand and, as the corresponding degrading enzyme, an endoribonuclease enzyme (RNase H) which specifically hydrolyzes RNA strands in DNA-RNA heteroduplexes[34,35] (**Figure 2a**). To demonstrate successful enzyme-driven strand replacement in the structure, we have labeled the RNA strand with Cy3 fluorophore and employed as a replacing strand a DNA oligonucleotide labeled with a Cy5 fluorophore (Figure 2b). We first show the successful assembly of scaffolds containing the RNA strand using fluorescence microscopy (Figure S1). Structures with an average length of 2.1 ± 0.1 μm and count of (27 ± 2) × 10^3 structures mm^{-2} are observed. Upon the addition of RNase H (5 U mL^{-1}) to a mixture containing the above scaffolds (0.25 μM) and the replacing DNA strand (0.35 μM), we observe a progressive replacement of the RNA strand over time as demonstrated by the increasing number of assembled green tiles (Cy5) and the consequent decrease of the red tiles (Cy3) (Figure 2c and S2). Decoration replacement is complete in 30 minutes, after which we obtain DNA-based scaffolds decorated with only Cy5-labels (Figure 2c-d). The rate of decoration replacement can be controlled by varying the concentration of RNase H enzyme in the range between 1 and 5 U mL^{-1} (Figure S3). Of note, in this range of enzyme concentrations, the average length (<L>, μm) and the total number of observed structures (<C>, number of structures mm^{-2}) remain constant during the decoration replacement, an observation that indicates that the decoration replacement process occurs without any structure disassembly (Figure 2e, solid dots). At higher RNase H concentrations (> 5 U mL^{-1}), on the contrary, we observe disassembly of the structures followed by re-assembly with the replacing strand (Figure S4). This could be attributed to the faster rate of RNA degradation compared to the rate of re-hybridization by the replacing strand. As control experiments, we also show that the strand replacement event does not proceed in the absence of the degrading enzyme (even after 24 hours) (Figure S5) and complete disassembly is obtained when the enzyme is added in the absence of the replacing strand (Figure 2e, empty dots and Figures S6-S7).

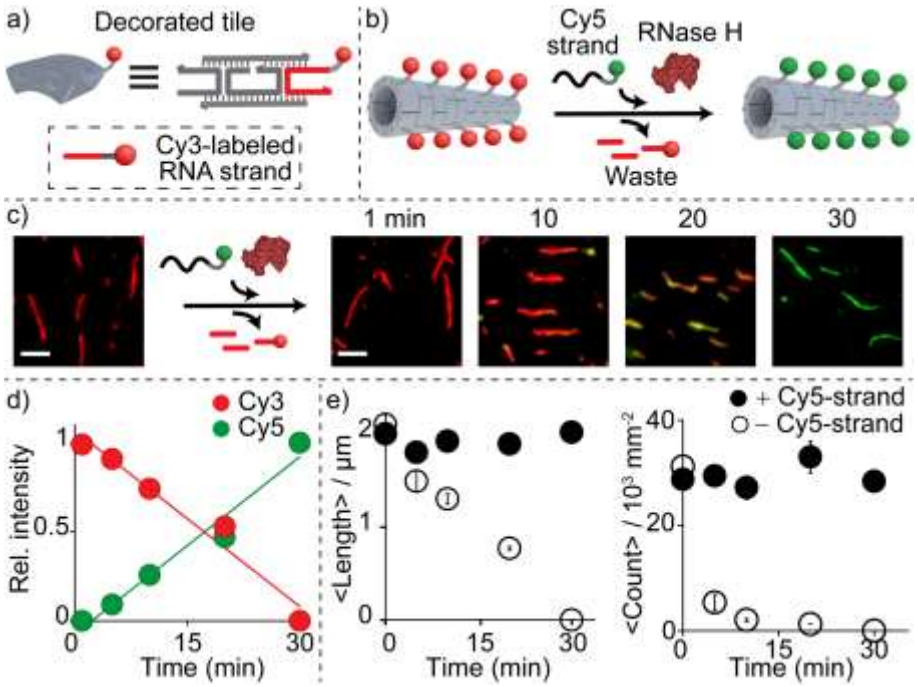

Figure 2. RNase H-driven dynamic decoration replacement in DNA-based scaffolds. *a) Cartoon of the DNA tile containing the Cy3-labeled RNA strand. b) RNase H-driven decoration replacement reaction scheme. c) Fluorescence microscope images showing the DNA scaffolds at the indicated time intervals after the addition of RNase H (5 U mL^{-1}). d) Relative intensities of the labels distributed along DNA structures at the indicated time intervals after RNase H addition (5 U mL^{-1}). e) Average length (<L>, µm) and count (<C>, number of structures mm^{-2}) of assembled structures. The experiments shown here were performed at 25 °C in 20 mM Tris-HCl, 10 mM $MgCl_2$, 1 mM EDTA, pH 8.0 buffer solution containing DNA tiles (0.25 µM), RNase H (5 U mL^{-1}) and, where indicated, DNA replacing strand (0.35 µM). Here and in the following figures average length and count values represent the average and error bars represent standard deviation based on triplicate measurements. Scale bar: 2.5 µm.*

2.2. UDG-Driven Decoration Replacement in DNA-Based Scaffolds

To demonstrate the versatility of our approach, we designed a DNA tile containing a labeled strand that can be replaced upon degradation by another enzyme. More specifically, as a degrading enzyme, we selected Uracil-DNA Glycosylase (UDG), a DNA repair enzyme belonging to the family of base excision repair (BER) that hydrolyses deoxyuridine mutations from ssDNA or dsDNA strands leading to the formation of abasic sites.[36,37] We have then designed a Cy3-conjugated strand in which 4 deoxyuridine lesions are uniformly distributed along the sequence (**Figure 3a**). The enzymatic activity of UDG on the mutated bases creates abasic sites where deoxyuridine lesions are present inducing the spontaneous de-hybridization of the strand and its downstream substitution by a replacing unmodified DNA strand labeled

with a Cy5 fluorophore (Figure 3b). We first confirmed the successful assembly of the structures from DNA tiles containing the deoxyuridine-modified strand with an average length of 2.7 ± 0.1 μm and count of (31 ± 3) × 10^3 structures mm^{-2} (Figure S8). The addition of UDG enzyme (50 U mL^{-1}) and a replacing DNA strand (0.35 μM) allows the progressive replacement of the deoxyuridine-containing strand over time as demonstrated by the increase in the number of assembled green tiles (Cy5) and the consequent decrease in the red ones (Cy3) (Figure 3c-d and Figure S9). The rate of decoration replacement can be further modulated by varying the concentrations of UDG in the range between 2 and 50 U mL^{-1} (Figure S10). Also, in this case, the average length (μm) and the total number of assembled structures (number of structures mm^{-2}) remain constant during the UDG-driven label replacement again supporting the hypothesis that decoration replacement occurs without prior scaffold disassembly (Figure 3e, solid dots). As a control experiment, we also demonstrated that the process of decoration replacement does not proceed in the absence of UDG (even after 48 hours) (Figure S11). Also, the UDG enzymatic activity in the absence of the replacing strand induces complete structural disassembly (Figure 3e, empty dots and Figure S12). The fact that both enzymes (RNase H and UDG) tested here gave comparable results in terms of strand degradation suggests that the target strand on the DNA scaffold is easily accessible by the enzyme. It is possible, however, that larger DNA- or RNA-degrading enzymes could have a more limited accessibility, a limitation that could require further optimization in the future.

We can reversibly control the decoration of DNA scaffolds with two different labels in the same solution. To demonstrate this, we employed tiles assembled with Cy3-labeled RNA strand and Cy5-labeled DNA strand containing 4 deoxyuridine lesions as the replacing strand. In the presence of RNase H, as expected, we observed the degradation of the Cy3-labeled RNA strand and the spontaneous replacement by the Cy5-labeled strand containing deoxyuridine. Upon the addition of the UDG enzyme and a second Cy3-labeled DNA strand, second replacement reaction proceeds, and the original decoration of the scaffolds (Cy3) is restored. We note that this second Cy3-labeled replacing strand is different from the original Cy3-labeled element (i.e. DNA instead of RNA). This is due to the fact that the solution contains RNase H (used for the first replacement process) and RNA-labeled strand would be degraded over time. Also in this case, the average length and the total number of assembled structures, also in this case, remain constant after the two replacement reactions (Figure 3f and S13).

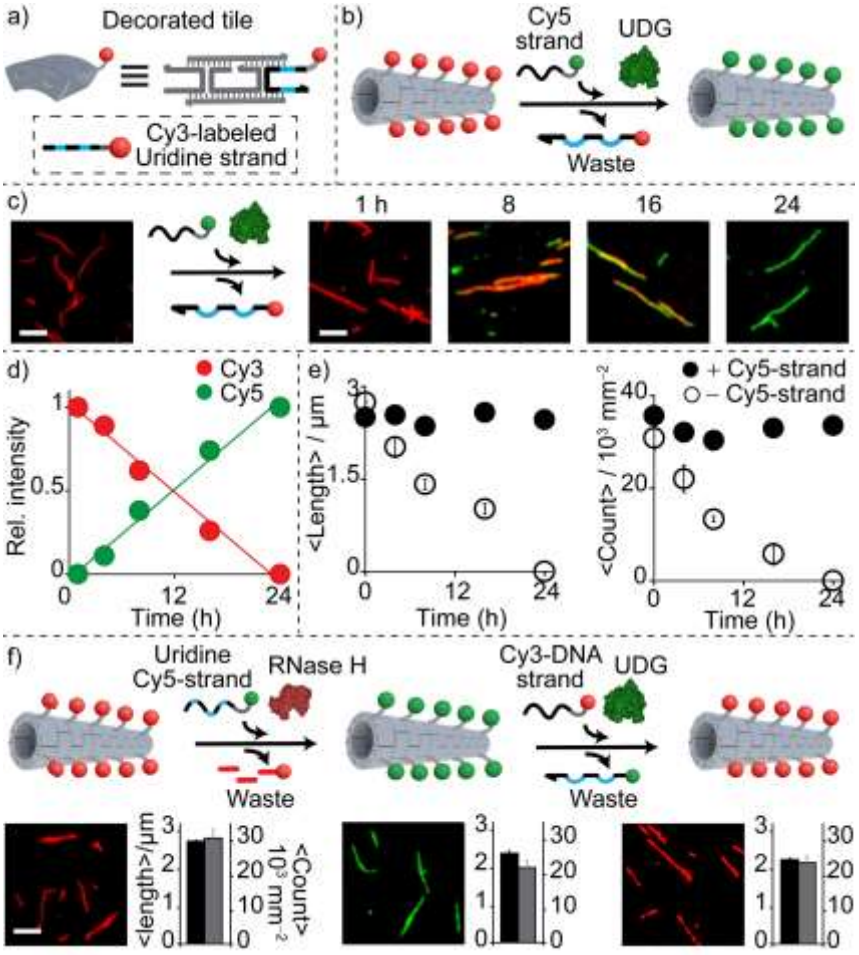

Figure 3. Uracil DNA Glycosylase (UDG)-driven dynamic decoration replacement in DNA-based scaffolds. *a) Cartoon of the DNA tile containing the Cy3-labeled DNA strand with 4 deoxyuridine lesions. b) UDG-driven decoration replacement reaction scheme. c) Fluorescence microscope images showing the DNA structures at the indicated time intervals after the addition of UDG (50 U mL^{-1}). d) Relative intensities of the labels distributed along DNA structures at the indicated time intervals after UDG addition (50 U mL^{-1}). e) Average length (<L>, µm) and count (<C>, number of structures mm^{-2}) of assembled structures during decoration replacement in the presence (solid dots) and absence (empty dots) of the replacing strand. f) Reversible decoration of DNA-based scaffolds scheme (top) and fluorescence images of decorated DNA structures obtained after each enzymatic reaction (bottom). The experiments shown here were performed at 25 °C in 20 mM Tris-HCl, 10 mM $MgCl_2$, 1 mM EDTA, pH 8.0 buffer solution containing DNA tiles (0.25 µM), UDG (50 U mL^{-1}) and, where indicated, DNA replacing strand (0.35 µM). Scale bar: 2.5 µm.*

2.3. Orthogonal Dynamic Decoration of DNA-Based Scaffolds

Our strategy allows to orthogonally control the distribution of different labels on DNA scaffolds from a solution containing multiple labels without crosstalk. To achieve this, we rationally engineered a DNA tile containing two enzyme-responsive strands: an RNA strand (red) and a deoxyuridine-DNA strand (black and blue) (**Figure 4a**). We first demonstrated the

successful assembly of DNA structures in the presence of both strands on the same tile (Figure S14). The assembled structures have an average length of 2.4 ± 0.2 µm and a count of (22 ± 2) × 10^3 structures mm^{-2}. We then added in the same solution two different DNA replacing strands, each conjugated to a different fluorophore (Cy3, Cy5) and each designed to replace one of the two enzyme-responsive strands in the tile. Upon addition of a single degrading enzyme (RNase H or UDG) or both enzymes, we can selectively guide the decoration on the DNA scaffolds in an orthogonal way without any crosstalk or significant FRET interactions between the two fluorophores (Figure 4b-c, Figures S15-S16). Also in this case, the average length and the total number of assembled structures remain unchanged (Figure 4d). Furthermore, by varying the ratio between the two labeled replacing strands, we can finely tune the decoration distribution of both labels in the DNA scaffolds (Figure 4e-g and Figure S17).

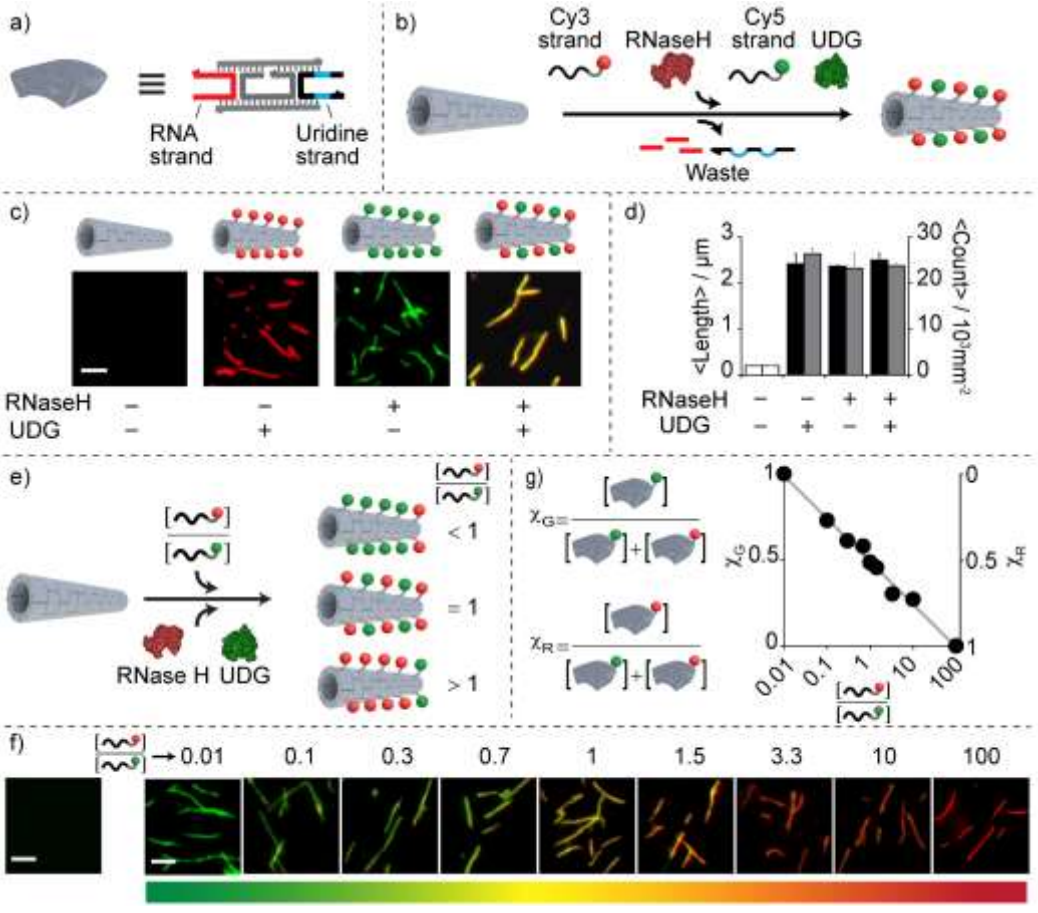

Figure 4. Orthogonal dynamic decoration of DNA-based scaffolds. *a) Cartoon of the DNA tile containing two enzyme-responsive strands: an RNA strand (red) and a deoxyuridine-DNA strand (black and blue). b) Orthogonal dynamic decoration of DNA-based scaffolds reaction scheme. c) Fluorescence microscope images of orthogonal decoration in the presence of a single or both enzymes. d) Average length (<L>, µm) and count (<C>, number of structures* mm^{-2}*) of assembled structures. e) Controlling label distribution on DNA scaffolds by varying*

the ratios of labeled replacing strands. f) Fluorescence microscope images of structures obtained at different ratios of labeled replacing strands. g) Plot of mole fraction of Cy5-labeled strands (χ_G) and Cy3-labeled strands (χ_R) in the assembled DNA structures. The experiments were performed at 25 °C in 20 mM Tris-HCl, 10 mM $MgCl_2$, 1 mM EDTA, pH 8.0 buffer solution containing DNA tiles (0.25 μM), RNase H (5 U mL^{-1}), UDG (50 U mL^{-1}) and DNA replacing strands (0.35 μM). Scale bar: 2.5 μm.

2.4. Dynamic decoration of DNA-Based Scaffolds with antigens

Dynamic and reversible decoration of DNA-based scaffolds is not only limited to the use of small fluorescent labels but can also be achieved with other more complex functional elements. To demonstrate this, we employed DNA strands conjugated with different antigens to achieve the dynamic control of antigen-decorated DNA structures. We first used assembled DNA tiles containing Cy3-labeled RNA strands and employed digoxigenin (Dig)-conjugated replacing DNA strands. Upon the addition of RNase H, Dig-decorated DNA scaffolds are observed following the colocalization of the fluorescent-labeled Anti-Dig antibody along the Dig-decorated DNA structures (**Figure 5a**-b and Figure S18). As expected, such antibody colocalization is not observed in the absence of RNase H (Figure 5b). Also, DNA scaffolds decorated with another antigen (i.e., dinitrophenol, DNP) are obtained employing the same tiles and a DNP-conjugated replacing strand. The decoration is once again confirmed by the addition of the corresponding fluorescent-labeled Anti-DNP antibody (Figure 5c-d and Figure S19). The strategy is versatile and similar results are also demonstrated by employing assembled tiles with Cy3-labeled deoxyuridine DNA strand and UDG as a corresponding degrading enzyme (Figure S20).

Our strategy allows the same DNA scaffold to undergo multiple decoration replacement reactions and display different functional moieties in a simple and dynamic way. To demonstrate this, we employed Cy3-decorated DNA tiles containing RNA strands and Dig-conjugated deoxyuridine as a replacing strand. The presence of RNase H, as expected, allows the first replacement reaction and we observe Dig-decorated structures (Figure 5e). Second replacement reaction proceeds upon the addition, to the same solution, of a DNP-conjugated DNA strand and UDG enzyme and, as a result, DNP-decorated scaffolds are observed (Figure 5e and Figure S21). Moreover our strategy can find applications in sensing multiple targets with the same scaffold with the expedient of dynamically changing the recognition element displayed on the surface of the scaffold. To demonstrate this we have initially employed DNA scaffolds decorated with Digoxigenin and coupled them with

fluorescent-labeled Anti-Dig antibody. Through a competition assay we can obtain information about the concentration of free Dig in solution (Figure S22). We then exchanged the recognition element on the same the addition using DNP-conjugated strand (as replacing strand) and UDG as degrading enzyme. The so-obtained DNP-decorated DNA scaffold can be then coupled with fluorescent-labeled Anti-DNP antibody and employed to measure DNP free in solution (Figure S23). A similar approach can also be used to detect Anti-Dig and Anti-DNP antibodies (Figures S24-S25).

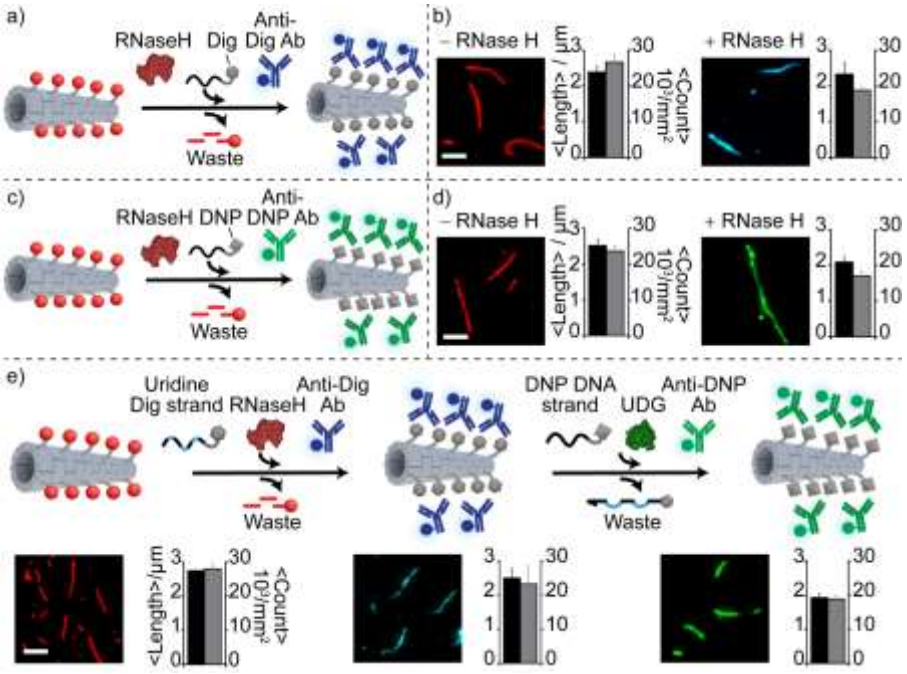

Figure 5. Dynamic decoration of DNA-based scaffolds with antigens. *a) Dig-decorated scaffolds reaction driven by RNase H. b) Fluorescence microscope images of Dig-decorated scaffolds obtained in the presence and absence of RNase H. c) DNP-decorated scaffolds reaction driven by RNase H. d) Fluorescence microscope images of DNP-decorated scaffolds obtained in the presence and absence of RNase H. e) Multiple decoration replacement reactions driven by RNase H and UDG. The experiments were performed at 25 °C in 20 mM Tris-HCl, 10 mM $MgCl_2$, 1 mM EDTA, pH 8.0 buffer solution containing DNA tiles (0.25 µM), RNase H (5 U mL^{-1}), UDG (50 U mL^{-1}), antigen-conjugated replacing strands (0.35 µM) and the corresponding fluorescent antibody (70 nM). Scale bar: 2.5 µm.*

Finally, we further investigated the possibility to orthogonally control the distribution of different antigens along the same DNA scaffold employing DNA tiles containing both enzyme-responsive strands (**Figure 6a**). To achieve this, we employed in the same solution two different DNA replacing strands, each conjugated to a different antigen (Dig, DNP) and

each designed to replace one of the enzyme-responsive strands in the tile (Figure 6b). The addition of a single degrading enzyme (RNase H or UDG) or both enzymes selectively guide the decoration of either a single or both antigens on the DNA scaffolds in an orthogonal way (Figure 6c-d, and Figure S26).

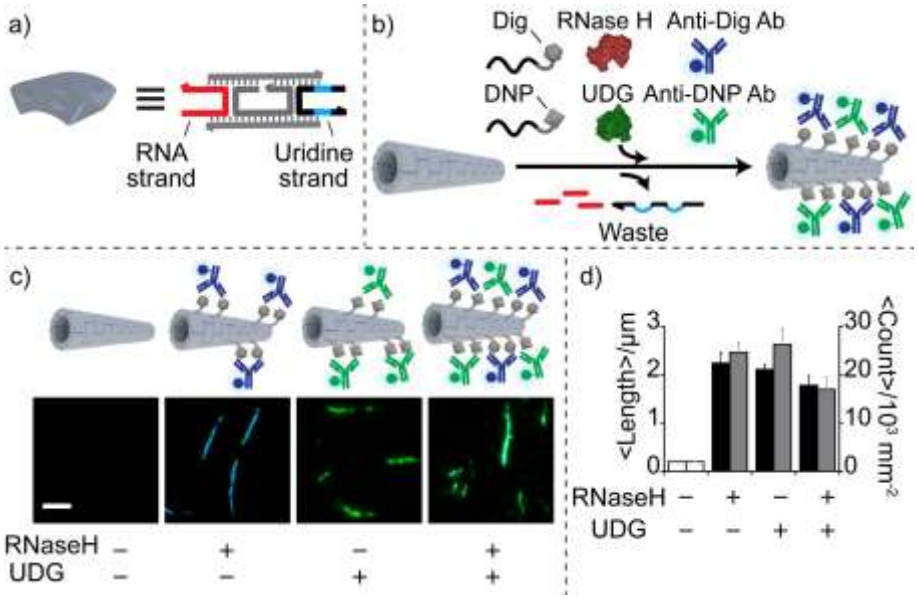

Figure 6. Orthogonal antigen decoration of DNA-based scaffolds. *a) DNA tile containing two different strands made of RNA and DNA containing deoxyuridine mutations. b) Orthogonal antigen decoration of DNA-based scaffolds reaction scheme. c) Fluorescence microscope images of orthogonal antigen decoration in the presence of a single or both enzymes. d) Average length (µm) and count (number of structures mm^{-2}) of assembled DNA structures. The experiments were performed at 25 °C in 20 mM Tris-HCl, 10 mM $MgCl_2$, 1 mM EDTA, pH 8.0 buffer solution containing DNA tiles (0.25 µM), RNase H (5 U mL^{-1}), UDG (50 U mL^{-1}), antigen-conjugated replacing strands (0.35 µM) and the corresponding fluorescent antibodies (70 nM). The error bars reflect the standard deviations of three separate measurements. Scale bar: 2.5 µm.*

3. Conclusion

In the last two decades, a variety of DNA-based structures, scaffolds, and assemblies that present an unprecedented level of precision in terms of shape and programmability have been described.[18,38] While the initial research efforts in this field were mostly dedicated to the demonstration of new self-assembly strategies to create more precise and complex 3D structures,[18,39] recently more focus has been devoted to the possible applications of these systems in real life.[26,40] In this regard, the possibility to functionalize DNA-based structures with labels, recognition elements, aptamers, and therapeutic drugs is of primary importance as it provides the required functionality to an otherwise inert structure. Functionalized DNA structures can thus serve as versatile tools for sensing, drug delivery, and imaging applications.[20,25,29] While several strategies have been proposed to date to decorate/functionalize DNA-based structures in a programmable way, finding new methods that guide the decoration event in a versatile and reversible way remains an unmet need.

In response to this, we have demonstrated here an enzyme-based strategy to dynamically control the decoration of DNA-based scaffolds. To do this, we selected two enzymes (Ribonuclease H (RNase H) and Uracil DNA Glycosylase (UDG)) and rationally engineered DNA tiles containing enzyme-responsive strands covalently conjugated to different molecular labels. The activity of the enzymes on their specific target strand induces strand de-hybridization from the tiles and the downstream decoration replacement by replacing strands conjugated to different labels. Of note, although the degraded strand is crucial for the structural stability of the DNA scaffolds, the enzyme-driven strand replacement occurs before the disassembly of the structure can be observed. We have also demonstrated the reversibility of the decoration replacement reactions and the possibility to orthogonally control the distribution of multiple labels on the same scaffold without crosstalk.

Our approach could offer the possibility to control the decoration of DNA-based structures with c (i.e., enzymes, small peptides, recognition elements, therapeutic agents, etc.) to achieve higher ordered molecular patterns[41,42] or to spatially organize enzymatic cascades.[43] We envision that this approach can be employed to induce functional changes in more complex DNA structures (including origami) providing diverse clinical and sensing applications.[30,41,44] Coupling this approach with other DNA-based temporally controlled systems[45,46] could also allow for dynamic control of the decoration of DNA structures over time and space.

4. Experimental Methods

Chemicals: All reagent-grade chemicals, including DEPC-treated water, $MgCl_2$, trizma hydrochloride, ethylenediaminetetraacetic acid (EDTA), NaCl, and 1,4-dithiothreitol (DTT), were purchased from Sigma-Aldrich (Italy) and used without further purifications. DyLight 488 goat polyclonal anti-Dig antibodies were purchased from Vector Laboratories (Burlingame, CA, USA) (cat#: Dl-7488), mouse monoclonal Alexa Fluor 647 anti-DNP antibodies were purchased from Santa Cruz Biotechnology (Heidelberg, Germany), (cat#: SC-69698). All the antibodies were aliquoted and stored at 4 °C for immediate use.

Enzymes: Uracil DNA Glycosylase (UDG), and Ribonuclease H (RNase H) were purchased from New England Biolabs (Beverly, MA, USA). Before use, RNase H (1000 U mL^{-1}) was activated by incubation for 1 h at 37 °C in 50 mM Tris−HCl buffer solution containing 50 mM KCl, 3 mM $MgCl_2$, and 50 mM DTT at pH 8.0.

Oligonucleotides: Oligonucleotides employed in this work were synthesized, labeled, and HPLC-purified by Biosearch Technologies (Risskov, Denmark) and Metabion International AG (Planegg, Germany) and used without further purification. The DNA oligonucleotides were dissolved in phosphate buffer 50 mM, pH 7.0, and stored at −20 °C until use. The RNA oligonucleotides were dissolved in DEPC-treated water and stored at −20 °C until use. All the sequences used are provided in the Supporting Information file.

Self-assembly of DNA scaffolds: The tile design and sequences in this study were described elsewhere.[31,32] DNA tiles for all the presented systems were prepared as follows. Each DNA tile strand was mixed at a final concentration of 5 μM in a 12 mM $MgCl_2$ solution. A 30-μL solution was annealed using a thermocycler (Bio-Rad Mastercycler Gradient) by heating the solution to 90 °C and cooling it to 25 °C at a constant rate for a 6-h period. The concentrations employed and buffer conditions for dynamic decoration of DNA scaffolds are reported in the caption of each figure. Detailed procedures employed are reported in the Supporting Information file.

Fluorescence imaging of DNA-based scaffolds: An Axio Scope A1 ZEISS microscope was used for fluorescence microscopy imaging. The images were acquired with a 100x oil objective and a monochrome CCD camera (Axiocam 503 mono-ZEISS). Images were analyzed and processed to correct for uneven illumination and superimposed to produce

multicolor images using ZEN-2 lite (ZEISS) software and ImageJ for analyzing the pixels intensity of the decorated structures. Average length and count of assembled scaffolds were quantified by image metrology using SPIP software (www.imagemet.com).

Statistical Analysis: All data shown in graphs are presented as mean ± standard deviation (SD). Statistical analysis was performed using GraphPad Prism 8 software. No specific preprocessing of data was performed prior to statistical analyses.

Acknowledgements

This work was supported by the European Research Council, ERC (project no. 819160) (F.R.), Associazione Italiana per la Ricerca sul Cancro, AIRC (project no. 21965) (F.R.), the Italian Ministry of University and Research (Project of National Interest, PRIN, 2017YER72K), and the European Union's Horizon 2020 research and innovation program under the Marie Skłodowska-Curie grant agreement No 896962, "ENZYME-SWITCHES" (E.D.G.).

References

[1] H. Cui, N. Pan, W. Fan, C. Liu, Y. Li, Y. Xia, K. Sui, *Adv. Funct. Mater.* **2019**, *29*, 1807692.

[2] S. Fuchs, K. Shariati, M. Ma, *Adv. Healthc. Mater.* **2020**, *9*, 1901396.

[3] M. Antonietti, S. Förster, *Adv. Mater.* **2003**, *15*, 1323.

[4] L. Zhang, J. M. Chan, F. X. Gu, J. W. Rhee, A. Z. Wang, A. F. Radovic-Moreno, F. Alexis, R. Langer, O. C. Farokhzad, *ACS Nano* **2008**, *2*, 1696.

[5] J. Borges, M. P. Sousa, G. Cinar, S. G. Caridade, M. O. Guler, J. F. Mano, *Adv. Funct. Mater.* **2017**, *27*, 1605122.

[6] H. Cui, M. J. Webber, S. I. Stupp, *Peptide Science* **2010**, *94*, 1.

[7] T. Aida, E. W. Meijer, S. I. Stupp, *Science* **2012**, *335*, 813.

[8] Z. Lei, Q. Wang, S. Sun, W. Zhu, P. Wu, *Adv. Mater.* **2017**, *29*, 1700321.

[9] Z. Lei, P. Wu, *Nat. Commun.* **2018**, *9*, 1.

[10] W. Qin, D. Ding, J. Liu, W. Z. Yuan, Y. Hu, B. Liu, B. Z. Tang, *Adv. Funct. Mater.* **2012**, *22*, 771.

[11] D. Wang, M. M. S. Lee, G. Shan, R. T. K. Kwok, J. W. Y. Lam, H. Su, Y. Cai, B. Z. Tang, *Adv. Mater.* **2018**, *30*, 1802105.

[12] B. P. Isaacoff, K. A. Brown, *Nano Lett.* **2017**, *17*, 6508.

[13] S. S. Lee, E. L. Hsu, M. Mendoza, J. Ghodasra, M. S. Nickoli, A. Ashtekar, M. Polavarapu, J. Babu, R. M. Riaz, J. D. Nicolas, D. Nelson, S. Z. Hashmi, S. R. Kaltz, J. S. Earhart, B. R. Merk, J. S. Mckee, S. F. Bairstow, R. N. Shah, W. K. Hsu, S. I. Stupp, *Adv. Healthc. Mater.* **2015**, *4*, 131.

[14] J. Leong, J. Y. Teo, V. K. Aakalu, Y. Y. Yang, H. Kong, *Adv. Healthc. Mater.* **2018**, *7*, 1701276.

[15] M. A. C. Stuart, W. T. S. Huck, J. Genzer, M. Müller, C. Ober, M. Stamm, G. B. Sukhorukov, I. Szleifer, V. v. Tsukruk, M. Urban, F. Winnik, S. Zauscher, I. Luzinov, S. Minko, *Nat. Mater.* **2010**, *9*, 101.

[16] M. Ikeda, T. Tanida, T. Yoshii, K. Kurotani, S. Onogi, K. Urayama, I. Hamachi, *Nat. Chem.* **2014**, *6*, 511.

[17] D. Samanta, S. B. Ebrahimi, C. A. Mirkin, *Adv. Mater.* **2020**, *32*, 1901743.

[18] N. C. Seeman, H. F. Sleiman, *Nat. Rev. Mater.* **2017**, *3*, 1.

[19] W. Engelen, C. Sigl, K. Kadletz, E. M. Willner, H. Dietz, *J. Am. Chem. Soc.* **2021**, *143*, 21630.

[20] M. Pfeiffer, K. Trofymchuk, S. Ranallo, F. Ricci, F. Steiner, F. Cole, V. Glembockyte, P. Tinnefeld, *iScience* **2021**, *24*, 103072.

[21] A. Kuzyk, Y. Yang, X. Duan, S. Stoll, A. O. Govorov, H. Sugiyama, M. Endo, N. Liu, *Nat. Commun.* **2016**, *7*, 1.

[22] K. Jahnke, V. Huth, U. Mersdorf, N. Liu, K. Göpfrich, *ACS Nano* **2021**, *16*, 7233.

[23] Q. Li, D. Zhao, X. Shao, S. Lin, X. Xie, M. Liu, W. Ma, S. Shi, Y. Lin, *ACS Appl. Mater. Interfaces* **2017**, *9*, 36695.

[24] S. M. Douglas, I. Bachelet, G. M. Church, *Science* **2012**, *335*, 831.

[25] C. Sigl, E. M. Willner, W. Engelen, J. A. Kretzmann, K. Sachenbacher, A. Liedl, F. Kolbe, F. Wilsch, S. A. Aghvami, U. Protzer, M. F. Hagan, S. Fraden, H. Dietz, *Nat. Mater.* **2021**, *20*, 1281.

[26] A. Monferrer, J. A. Kretzmann, C. Sigl, P. Sapelza, A. Liedl, B. Wittmann, H. Dietz, *ACS Nano* **2022**, *doi: 10.1021/acsnano.1c11328.*

[27] B. Saccà, R. Meyer, M. Erkelenz, K. Kiko, A. Arndt, H. Schroeder, K. S. Rabe, C. M. Niemeyer, B. Saccà, D.-C. R. Meyer, D.-B. M. Erkelenz, M. K. Sc Kiko, A. Arndt, H. Schroeder, K. S. Rabe, C. M. Niemeyer, *Angew. Chem. Int. Ed.* **2010**, *49*, 9378.

[28] R. Ibusuki, T. Morishita, A. Furuta, S. Nakayama, M. Yoshio, H. Kojima, K. Oiwa, K. Furuta, *Science* **2022**, *375*, 1159.
[29] J. M. Stewart, M. Viard, H. K. K. Subramanian, B. K. Roark, K. A. Afonin, E. Franco, *Nanoscale* **2016**, *8*, 17542.
[30] S. Li, Q. Jiang, S. Liu, Y. Zhang, Y. Tian, C. Song, J. Wang, Y. Zou, G. J. Anderson, J. Y. Han, Y. Chang, Y. Liu, C. Zhang, L. Chen, G. Zhou, G. Nie, H. Yan, B. Ding, Y. Zhao, *Nat. Biotechnol.* **2018**, *36*, 258.
[31] P. W. K. Rothemund, A. Ekani-Nkodo, N. Papadakis, A. Kumar, D. K. Fygenson, E. Winfree, *J. Am. Chem. Soc.* **2004**, *126*, 16344.
[32] D. Y. Zhang, R. F. Hariadi, H. M. T. Choi, E. Winfree, *Nat. Commun.* **2013**, *4*, 1.
[33] L. N. Green, H. K. K. Subramanian, V. Mardanlou, J. Kim, R. F. Hariadi, E. Franco, *Nat. Chem.* **2019**, *11*, 510.
[34] S. Agarwal, E. Franco, *J. Am. Chem. Soc.* **2019**, *141*, 7831.
[35] S. M. Cerritelli, R. J. Crouch, *FEBS J* **2009**, *276*, 1494.
[36] N. Farag, G. Ercolani, E. del Grosso, F. Ricci, *Angew. Chem. Int. Ed.* **2022**, *61*, e202208367.
[37] H. E. Krokan, M. Bjørås, *Cold Spring Harb. Perspect. Biol.* **2013**, *5*, a012583.
[38] M. R. Jones, N. C. Seeman, C. A. Mirkin, *Science* **2015**, *347*
[39] A. M. Mohammed, P. Šulc, J. Zenk, R. Schulman, *Nat. Nanotechno.* **2016**, *12*, 312.
[40] I. Seitz, H. Ijäs, V. Linko, M. A. Kostiainen, *ACS Appl. Mater. Interfaces* **2022**, *14*, 38515.
[41] P. S. Kwon, S. Ren, S. J. Kwon, M. E. Kizer, L. Kuo, M. Xie, D. Zhu, F. Zhou, F. Zhang, D. Kim, K. Fraser, L. D. Kramer, N. C. Seeman, J. S. Dordick, R. J. Linhardt, J. Chao, X. Wang, *Nat. Chem.* **2019**, *12*, 26.
[42] J. Fu, Y. R. Yang, A. Johnson-Buck, M. Liu, Y. Liu, N. G. Walter, N. W. Woodbury, H. Yan, *Nat. Nanotechno.* **2014**, *9*, 531.
[43] J. Fu, M. Liu, Y. Liu, N. W. Woodbury, H. Yan, *J. Am. Chem. Soc.* **2012**, *134*, 5516.
[44] A. Keller, V. Linko, *Angew. Chem. Int. Ed.* **2020**, *59*, 15818.
[45] J. Bucci, P. Irmisch, E. del Grosso, R. Seidel, F. Ricci, *J. Am. Chem. Soc.* **2022**, *144*,43.
[46] L. Heinen, A. Walther, *Sci. Adv.* **2019**, *5*, 7.

We demonstrate an enzyme-based approach to decorate DNA-based scaffolds in a dynamic and reversible way. Enzyme-responsive strands in the assembled scaffolds undergo degradation and spontaneous replacement by strands decorated with different labels in the presence of their corresponding enzymes.

N. Farag, M. Đorđević, E. Del Grosso*, F. Ricci*

Dynamic and Reversible Decoration of DNA-Based Scaffolds